ELSEVIER

Polymer 44 (2003) 773–782

polymer

www.elsevier.com/locate/polymer

Influence of pre-shearing on the crystallisation of conventional and metallocene polyethylenes

Choon K. Chai[a,*], Quentin Auzoux[a], Héry Randrianatoandro[a], Patrick Navard[b], Jean-Marc Haudin[b]

[a]*BP Chemicals, Research and Technology Centre, Ecopolis Lavera Sud, Boîte Postale no. 6, 13117 Lavéra, France*
[b]*Ecole des Mines de Paris, Centre de Mise en Forme des Matériaux (CEMEF), UMR CNRS 7635, Boîte Postale no. 207, 06904 Sophia Antipolis Cedex, France*

Received 20 May 2002; accepted 25 October 2002

Abstract

The influence of pre-shearing on the crystallisation of a conventional *Ziegler–Natta* catalysed and a *metallocene* catalysed linear low-density polyethylene (LLDPE) samples was studied by a rheo-optical method, coupling light scattering and steady shear flow. Experiments were performed on a high-temperature shearing cell, with a pair of parallel quartz plate windows. The polymers were sheared at a melt temperature T_s (ranging from 190 to 150 °C) at a constant shear rate ($\dot{\gamma}$) for a duration time t_s. After cessation of shear (at a given deformation of $\dot{\gamma}t_s$ unit), the sample was maintained at the selected melt temperature for a waiting time t_w (ranging from 0 to 10 min) before it was cooled down to 90 °C. Small-angle light scattering (SALS) patterns were recorded during the whole process. It was shown that the pre-shear history thus investigated has no measurable influence on crystallisation of the linear metallocene LLDPE. For the Ziegler–Natta sample, the influence of pre-shear on its crystallisation is larger when the shear rate ($\dot{\gamma}$) and strain ($\dot{\gamma}t_s$) are large, the waiting time t_w is smaller or the temperature T_s is lower. The consequence of shear is giving ellipsoidally deformed spherulites, elongated in the flow gradient direction, which originate from oriented nuclei. Crystallisation, following flow in particular, is shown to be a very good probe of chain orientation and it turns out to be more sensitive than classical linear rheological methods. It can detect if the sheared sample is in a steady state or if all chains have relaxed after a flow. For example, it is surprisingly shown that chain orientation for the Ziegler–Natta sample requires a large amount of shear deformation, in the order of 1000 strain units, to reach a steady state.

Keywords: Crystallisation; Light scattering; Metallocene

1. Introduction

Crystallisation is an important physical process in polymer science for both fundamental and technological reasons. It is kinetically controlled and involves the transportation of molecules from the disordered liquid phase to the ordered solid phase. It can be sub-divided into three stages: nucleation, growth and the perfection of the interior crystalline structure of the crystalline regions (or secondary crystallisation). The nucleation process for quiescent polymers melt can usually be described by a Poisson point process, while with the influence of flow, nuclei can be created by flow-induced orientation phenomena in the melt. The subsequent growth is strongly dependent on thermo-mechanical history; otherwise growth takes place radially in the form of spherical entities (spherulites).

Among all the polymers studied, polyethylene has a special place. Its apparent structural simplicity, low melting temperature, easiness to prevent degradation and economical importance has attracted numerous studies that describe its quiescent crystallisation behaviour. For instance, the internal morphology of polyethylene spherulites was elucidated [1] as far back as 1955 and polyethylene single crystals were prepared by three different groups [2–4] in 1957. The theories for nucleation [5,6] and growth [5–8] were mainly applied to this polymer.

However, during thermoplastic processing (e.g. film blowing) polymer crystallisation in general is rarely

* Corresponding author. Tel.: +33-4-42-42-94-47; fax: +33-4-42-42-94-45.
E-mail address: chaic@bp.com (C.K. Chai).

0032-3861/03/$ - see front matter © 2002 Elsevier Science Ltd. All rights reserved.
PII: S0032-3861(02)00773-5

occurring at rest, but during or just after a flow. It is strongly influenced by the thermo-mechanical history during processing: if the strain experienced was sufficiently large, nuclei become thread-like and grow mainly perpendicular to the thread, leading to a shish–kebab structure. Pennings et al. [9] obtained polyethylene shish–kebabs from dilute solutions under elongational flow. At the same time, Keller [10,11] proposed the model of row-nucleated morphologies for crystallisation of polyethylene from stressed melts. These two types of morphology are nowadays considered as identical.

The commercial importance of this flow-induced crystallisation, which occurs in most processes associated with orientation, in the processing of polyethylene has long been recognised as its vast range of properties have been exploited through molecular chain orientation and perfection of crystalline phase. Nevertheless, understanding the mechanisms of flow-induced crystallisation is not an easy task. In the 1970s, a great effort was devoted to elucidate the fibre formation under elongation flow from dilute solutions of polymers [9]. Shear flow was often neglected as it was considered at that time as a 'weak' flow, unable to provide chain extension and to induce fibre formation [9,12]. However, in polymer melts even shear flow modifies the crystallisation behaviour and this of prime importance for polymer processing. First of all, it has been recognised, for a long time for various polymers including polyethylene that the crystallisation is considerably accelerated by shear [13–30]. Most of the first experiments used custom-made rheometers and were concerned with the measurement of the induction time of crystallisation [13,16,17,19,20], because the onset of crystallisation is relatively easy to characterise by an increase of the force or the transmitted torque. Some studies [17,18,21,22] determined the fraction of transformed material versus time. But, at the beginning only few in situ measurements concerned the density of nuclei formed under shear and growth rate of the subsequent morphologies [22]. After this pioneering period, in situ crystallisation experiments have been generalised. They combine a model shear experiment (parallel plate [25,26,30], rotational plate–plate [23,24,28], fibre pull-out [29,31–33], die extrusion [34,35]) and a physical probe of the structure development, e.g. measurement of transmitted light [26,35], optical microscopy [26,30–33], X-ray diffraction [36], and Raman [37].

We have previously used Rheo-X-ray and Rheo-Raman techniques [36,37] for the studies of flow-induced orientation and crystallisation on high-density polyethylene melts. The overall objective of this series of work is to investigate the effects of molecular structure on flow-induced orientability of polymer chains during processing and how the latter influences the crystallisation kinetics during subsequent cooling, leading to its modification of the solid-state morphology and orientation which, in turn, have a strong impact on physical properties (e.g. optical and mechanical).

The objective of this paper is to quantitatively describe how a pre-shear history is influencing the crystallisation of two high alpha olefins copolymers of similar melt index and density, but of different molecular weight distributions (MWD). The first is a conventional *Ziegler–Natta* catalysed linear low-density polyethylene (LLDPE), hexene-copolymer, named as PE3. The second is a linear *metallocene* hexene-copolymer, labelled as PE1. Both have similar molecular weights, but PE3 is broader in molecular weight distribution (MWD) and has a larger proportion of long chains (high molecular weight fraction) than PE1.

In general, metallocene LLDPE has a more homogeneous chemical composition and narrower molecular weight distribution than Ziegler–Natta catalyst LLDPE. These changes at the molecular scale induce major differences in melt rheology, crystallisation kinetics (especially during flow) as well as solid-state properties that, in turn, affect the film blowing process and film properties. For instance, it is known that films made from metallocene LLDPE show superior mechanical properties than the 'conventional' Ziegler–Natta (Z–N) LLDPE. On the other hand, the reduced shear thinning behaviour linked with its narrower molecular weight distribution leads to limitation in melt pressure, melt fracture and bubble stability.

Though both catalyst types produce semi-crystalline polymers consisting of a crystalline and an amorphous phase, it is difficult to control and predict the Z–N product molecular structures that dictate the concentration of tie chains thus created in the polymer during crystallisation process, such that balanced product properties are obtained. Tie chains are polyethylene chains in which part of the chain has been crystallised into a lamellar crystal and part has been rejected due to a short-chain branch imperfection. This part of the rejected chain can then be incorporated into another crystal, and thus, a tie chain is formed between the crystals. An important benefit of tie chains is increased polymer toughness, manifested as higher impact resistance and mechanical properties in the products.

These two samples were submitted to the same shear histories. We studied the influence of the shear temperature; shear rate, duration of shear, waiting time between the cessation of steady shear and the cooling, on their crystallisation behaviours. Crystallisation was studied by small-angle light scattering (SALS). All the experiments were conducted in a high-temperature transparent shear device. We will show that the crystallisation is a very sensitive probe of chain orientation and thus can be used as a rheological tool.

2. Experimental

2.1. Resin characterisation

The melt flow rate (MFR) of the polymers was measured

under conditions that conform to ISO 1133 (1991) and BS 2782:PART 720A (1979) procedures. The weight of polymer extruded through a die of 2.095 mm diameter, at a temperature of 190 °C, during a 600 s time period and under a standard load of 2.16 kg is recorded. The polymer densities were measured according to ISO-1872/1 test method.

The apparent molecular weight distribution and associated averages (M_w and M_n) of the polymers, uncorrected for long chain branching, were determined by gel permeation chromatography [38] using a Waters 150CV. The solvent used was 1,2,4 trichlorobenzene at 145 °C, stabilised with 0.05% BHT. The nominal flow rate was 1 ml/min. Solutions of concentration 0.05–0.1% (w/w) were prepared at 155 °C for 1.5–2 h with stirring, and the nominal injection volume was set at 250 ml. 3 Shodex AT80 M/S columns were used with a plate count (at half height) of typically 23,000. The differential refractometer detector alone was used for these studies. Calibration was achieved using broad molecular weight linear polyethylene standards with a correction for dispersion broadening. This calibration has been checked against a NIST certified polyethylene SRM1475 standard.

Rheological measurements were carried out on a Rheometrics RDS-2 with 25 mm diameter parallel plates in the dynamic mode at 190 °C. A strain sweep (SS) experiment was initially carried out to determine the linear viscoelastic strain that would generate a torque signal that is greater than 10% of the full scale (2000 g cm) of the transducer over the full frequency (e.g. 0.01–100 rad/s) range. This is also to ensure that the selected applied strain is well within the linear viscoelastic region of the polymer so that the oscillatory rheological measurements do not induce structural changes to the polymer during testing. This procedure was carried out first for all the samples. Frequency sweep experiments at 190 °C and 15% strain in parallel plate mode were then run under nitrogen from 0.01 to 100 rad/s.

Analytical temperature rising elution fractionation [39] (TREF) experiments were also carried out to measure the distribution of short-chain branching (SCBD) of these copolymerised samples. A chromatographic pump was used to provide a constant flow of solvent through a stainless steel column (length 300 mm and diameter 7 mm) which was packed with 200 μm glass beads and held in a thermo-regulated oven. The polymer eluted was detected with an infrared detector set at a wavelength of 3.48 μm. The solvent used was 1,2,4-trichlorobenzene (TCB) stabilised with 500 ppm BHT antioxidant. Polymer was loaded into the column by injecting ~10 ml of a 0.2% (w/v) solution. The column was then cooled from 140 °C to room temperature at 2 °C/min. The column was heated at a rate of 20 °C/h until the entire polymer had been eluted from the column.

2.2. Rheo-optical shear and crystallisation experiments

The rheo-optical shear experiments were conducted in a high-temperature transparent parallel disk shearing cell, manufactured by Linkam Scientific, Epsom, Surrey, UK. The 25 mm diameter sample disk is placed between two circular quartz windows, which are in close thermal contact within two (upper and lower) silver block heaters. The temperature range of this flow cell is between ambient and 400 °C, with a temperature control better than ±0.5 °C and a shear rate range of 0.05–100 s^{-1}. The gap between the windows can be varied from 10 to 2500 μm and is controlled by a second stepper motor.

The shear cell was mounted on a vertical bench equipped with a He–Ne laser (of wavelength $\lambda = 632.8$ nm), two polarisers, a screen and a CCD camera. The SALS patterns were analysed using IPAS software (commercialised by Laser Instrument Diffusion, 495 route de la Mer, 06410 Biot, France), which is capable of performing averaging and size calculations. The size of the PE spherulites was simply deduced from the crossed-polariser (HV) pattern [40], by averaging the intensity versus scattering angle over the four lobes.

The experimental procedure for the pre-sheared then crystallisation is as follows. The specimen was compression-moulded at 190 °C from pellets and slow cooled to room temperature in the press under pressure. The 25 mm diameter sample is then positioned between the two quartz plates of the Linkam cell, previously heated at 190 °C, under a nitrogen flow. The sample is left at this temperature for ~15 min. The cell is then brought to the test temperature T_s (190, 170 and 150 °C) and equilibrated for an additional ~5 min (except in the cases of $T_s = 190$ °C) to ensure good temperature stabilisation. The LLDPE melt is then sheared at a given shear rate $\dot{\gamma}$ (which ranges from 1 to 18 s^{-1}) for a shearing time, t_s. After cessation of shear (i.e. at a given strain history, $\dot{\gamma}t_s$), the sample was maintained at this selected test temperature (T_s) for a waiting time, t_w (ranging from 0 to 10 min) before it was cooled down to 90 °C, at a controlled cooling rate of 20 °C/min. Light scattering patterns were recorded during the whole process.

3. Results and discussion

3.1. Polymer structure characterisation

Fig. 1 shows the molecular weight distribution as obtained by GPC and Table 1 summarises the molecular characteristics of the two samples. The linear metallocene C6-copolymerised PE1 has a weight average molecular weight (M_w) of ~1.0×10^5 g/mol and a molecular weight distribution (M_w/M_n) of 2.4; while the conventional Ziegler–Natta catalysed C6-copolymerised PE3 is broader in molecular weight distribution ($M_w/M_n = 3.1$) but has a similar M_w as PE1. The notable molecular structure

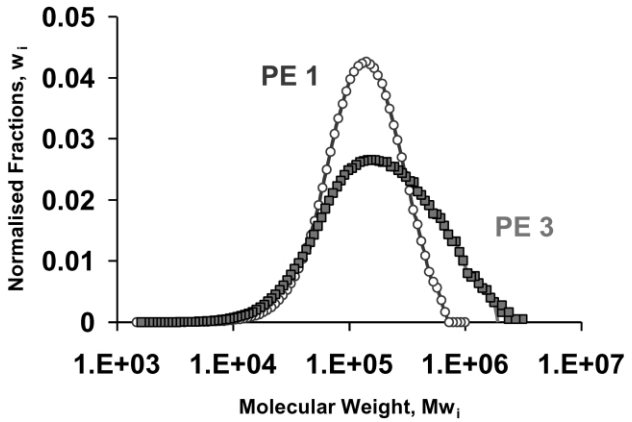

Fig. 1. Molecular weight distribution obtained by GPC of the two LLDPE samples.

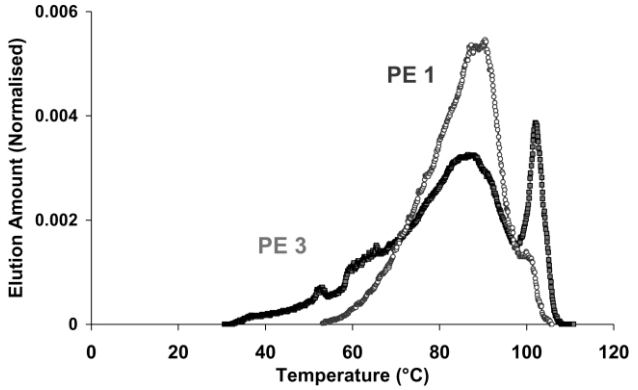

Fig. 2. TREF data for metallocene and Ziegler–Natta LLDPEs, PE1 and PE3, respectively. All plots are normalised for unit area. Note the bimodal composition distribution and lesser composition homogeneity for PE3.

difference between them is the presence of a high molecular weight tail (a small fraction of longer chains as indicated by the higher moment of the molecular weight distribution, M_z, (Table 1) in the PE3 Ziegler–Natta sample. The contribution of these longer molecular chains during shearing and its drastic influence on the crystallisation behaviour will be shown later.

Fig. 2 shows the TREF data for the metallocene and Ziegler–Natta LLDPEs, PE1 and PE3, respectively. It clearly shows that the conventional Ziegler–Natta catalysts produce a PE3-type polymer of heterogeneous composition and broad MWD (Fig. 1), with a bimodal composition distribution. The high-temperature TREF peak, at $T > \sim 97$ °C, is associated with a significant fraction of larger molecules that are rather narrowly distributed and practically without short-chain branches (high-density fraction).

In contrast, metallocene catalysts provide polymers with a homogeneous composition, giving narrower molecular weight distribution (Fig. 1) and narrow comonomer distribution, as shown in Fig. 2 for PE1 where its TREF plot can be described by a rather broad peak and a second small peak at $T > \sim 97$ °C. Thus, the metallocene PE1 tends to melt over a narrower temperature range and at a lower temperature than the Ziegler–Natta PE3.

3.2. Linear dynamic rheology

Fig. 3(a) and (b) show the plots of the moduli ($G'(\omega), G''(\omega)$) and the magnitude of the complex viscosity $\eta^*(\omega)$ against frequency (ω) for PE1 and PE3 at 190 °C. Fig. 3(a) highlights that the experimentally lowest accessible dynamic moduli of these industrial resins are far from terminal region, as their $d[\log G'(\omega)]/d[\log G''(\omega)] < 2$ (viz. 1.55 for PE1 and 1.35 for PE3, suggesting the latter possesses higher fraction of longer chains). The differences in the flow curves between PE1 and PE3 in Fig. 3(b) clearly demonstrate the influence of molecular weight distribution (MWD) broadening in improving the processability of the latter, with a large increase in low shear rate viscosity and stronger shear thinning at high shear rates.

Fig. 3(c) shows the relaxation times spectra, analysed using a commercially available IRIS™ software package that is based on a non-linear regression [41] to determine the best set, with minimum number, of Maxwell parameters (g_i, λ_i), for PE1 and PE3. The plot shows that the relaxation times spectrum of PE3 spans to longer relaxation times than PE1, consistent with the GPC data (Fig. 1), showing that the Ziegler–Natta sample contains a higher fraction of longer chains. This is further shown by the increase in its effective characteristic relaxation times (λ_w), calculated from the ratio of the zero shear rate viscosity to the plateau modulus, and the longest relaxation times (λ_{max}), as given in Table 1.

3.3. Influence of shear rate (at constant deformation) on the subsequent crystallisation

Without imposing a shear rate (i.e. with the shear time $t_s = 0$), and cooling down at 20 °C/min, the two polymers crystallise under cooling in the form of a spherulitic texture.

Table 1
Summary of molecular structure parameters, by GPC and linear rheology, for PE1 and PE3

Molecular structure parameters	PE1 (metallocene LLDPE)	PE3 (Ziegler–Natta LLDPE)
M_w (g/mol)	9.5×10^4	1.0×10^5
M_z (g/mol)	1.7×10^5	2.9×10^5
M_w/M_n	2.4	3.1
λ_w (s)	0.02	0.05
λ_{max} (s)	2.8	27.3

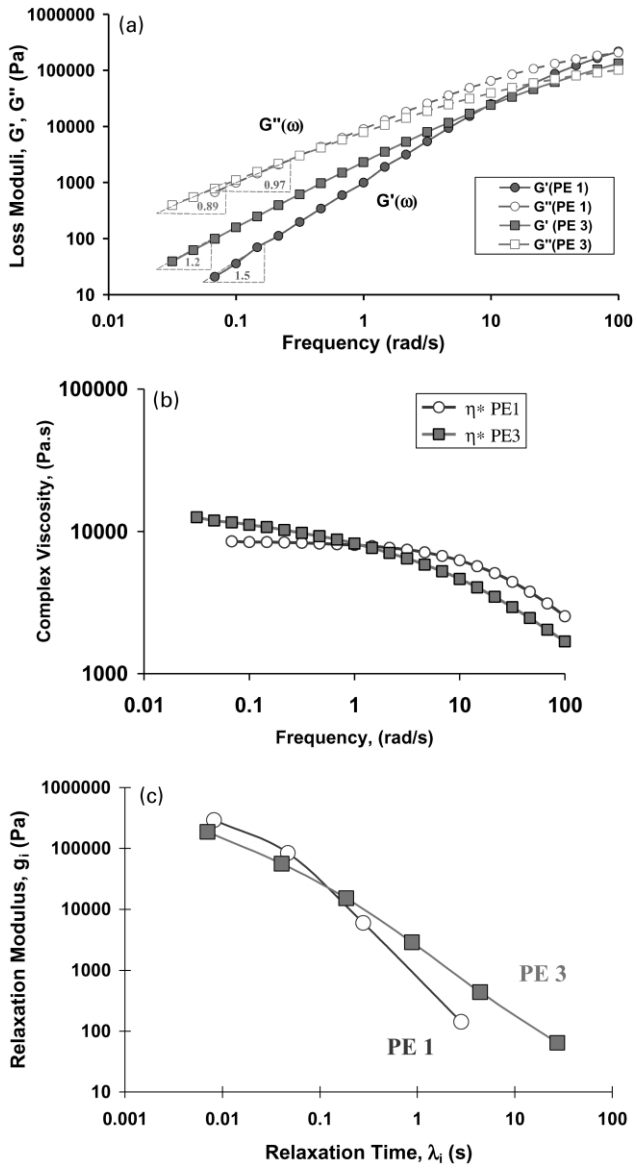

Fig. 3. (a) The storage (G') and loss (G'') moduli as a function of frequency for PE1 and PE3 at 190 °C. (b) The magnitude of complex viscosity as a function of frequency for PE1 and PE3 at 190 °C. (c) The relaxation spectra for PE1 and PE3 at 190 °C.

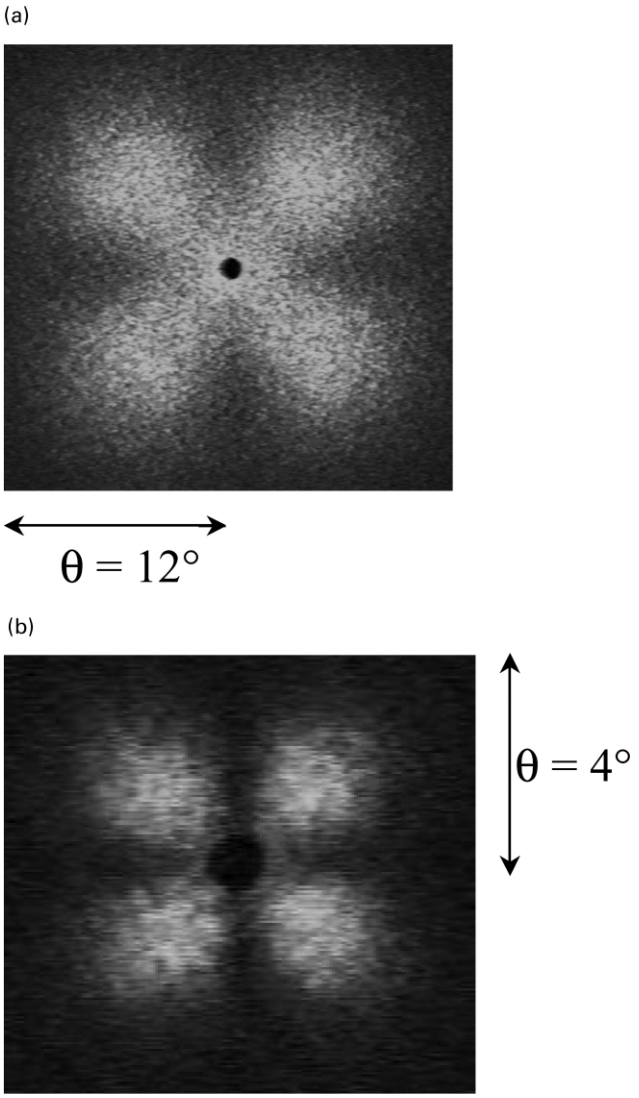

Fig. 4. The four lobes SALS scattering patterns of (a) PE1 and (b) PE3 recorded under zero shearing conditions.

Their actual crystallisation processes are different and complex, with several stages. They are not the subjects of the present study. However, the mean initial radius (R_0) of these spherulites is found to be ~3 μm for the metallocene PE1 and ~12 μm for Z–N PE3 sample, as calculated by averaging the intensity versus scattering angle (θ) over the four lobes from the SALS pattern [40], as shown in Fig. 4(a) and (b), respectively.

The influences of shear rate, at constant strain ($\dot{\gamma}t_s$) of 360 units, on the final size of the spherulites for both polymers are discussed below.

3.3.1. PE1 at $T_s = 190$ °C

With a waiting time (t_w) of just 2 s, the result in Fig. 5(a) showed that there is clearly no pre-shear effect on the crystallisation of the metallocene PE1 sample. This is because 2 s are of the order of the largest relaxation time for this polymer. In fact, for all the three studied temperatures ($T_s = 190$, 170 and 150 °C), we did not observed any significant influence of the pre-shear on the subsequent crystallisation of metallocene PE1. The absence of longer chains gives a fast molecular disorganisation at the end of the flow that leads to a lack of flow memory when the narrower MWD metallocene PE is crystallising.

3.3.2. PE3 at $T_s = 190$ °C

The Ziegler–Natta catalysed sample shows a very different behaviour in Fig. 5(b). The influence of shear at short waiting times is pronounced. The apparent radius of the spherulites is decreasing. However, this decrease becomes less pronounced when the waiting time is increased. Above a waiting time of 480 s, there does not

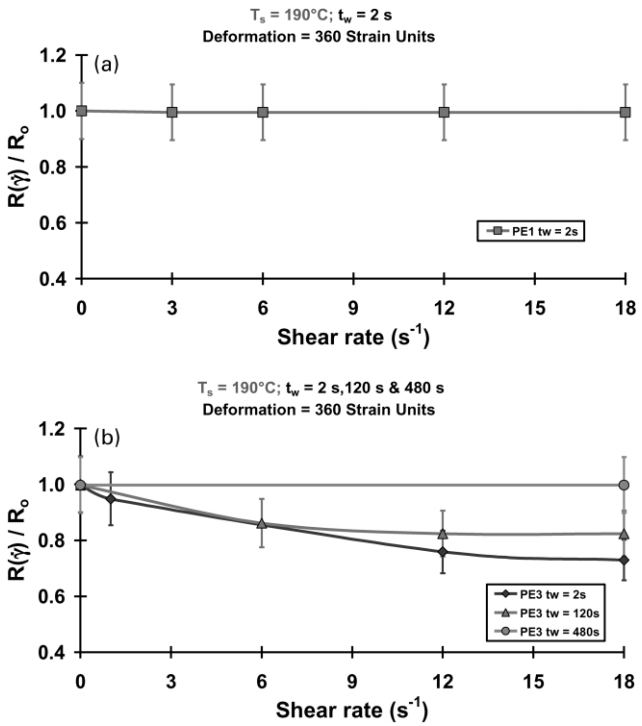

Fig. 5. Spherulite radius $R(\dot{\gamma})$ divided by the radius without shear R_0 versus applied shear rate for (a) PE1, and (b) PE3 when sheared at 190 °C, with varying length of the waiting times, t_w. The total deformation during shear is the same for all shear rates, i.e. $(\dot{\gamma}t_s) = 360$ shear units.

appear to have any influence of shear on the spherulites size of PE3, whence the polymer could have fully relaxed its orientation/deformation memory. Thus, it suggests that the waiting time $t_w \sim 480$ s appears to represent the largest relaxation time of the PE3 sample. This is considerable longer (~20 times) than the longest relaxation time ($\lambda_{max} \sim 27$ s) experimentally accessible by linear dynamic rheology analysis, since it is far from terminal region with its $d[\log G'(\omega)]/d[\log G''(\omega)] = 1.35$, as shown in Fig. 3 and Table 1. Alternatively, the extrapolation of the shear thinning portion of the viscosity curve at a shear rate corresponding to reciprocal of 480 s in Fig. 3(b) gives an estimate of the dynamic shear viscosity of PE3, i.e. 13,600–14,800 Pa s (as compared with 8500 Pa s for PE1). This is 1.6–1.7 times larger than the viscosity of the PE1 sample, stressing the great importance of the very long chains.

Next, one should ask what is the morphology of the sheared sample. Does a smaller radius mean a larger amount of spherulites? In fact, one has to remember that the scattering experiment probes the shear direction—vorticity plane, with no information in the gradient direction, i.e. in the sample thickness. In order to probe this direction, the following experiment was performed on PE3 (as schematically shown in top diagram of Fig. 6). During cooling from 190 °C, when the polymer is starting to crystallise, a very slow relative displacement of the two plates of the shear cell was imposed to the sample. Its consequence was to distort *reversibly* the SALS pattern (as illustrated in the middle and bottom diagrams of Fig. 6), which was then elongated in the vorticity direction. This clearly indicated that the sheared polymer crystallised in an oriented manner, with a faster spherulitic growth along the gradient direction, the two other directions having the same growth rate. It is because of these equal rates that the SALS pattern probed in the flow direction—vorticity plane has four equally spaced lobes. The spherulite radius, as shown in Fig. 5 (and later in Figs. 7–9), is thus the radius of the small axis of the ellipsoidal morphology.

For the PE3 sample, birefringence and stress appear to relax in less than ~20 s after having imposed a shear in the shear rate range used here [42]. This shows that most of the polymer chains are relaxed except for a very small fraction of longer chains that relax in a few hundred seconds. This small fraction of elongated chains that is keeping the memory of orientation may act as nuclei. It has been recently observed by in situ X-ray scattering experiments that chains oriented during flow are acting as nuclei and that their initial orientation (along the flow direction) is driving the orientation of the subsequent crystallisation [43]. The same is found here by SALS. What is new here is the clear difference between metallocene and Ziegler–Natta LLDPEs, stressing the importance of longer chains in the nucleation and orientation processes of polymer crystallisation, as soon as a flow is involved. Another point of interest is to note that these nuclei dictate that the direction perpendicular to them, in the shear gradient direction, will have the fastest crystallisation rate.

The preferential growth of the lamellar crystals perpendicular to the flow direction is often mentioned in the literature [44], but there exits only few data concerning the anisotropy of growth rate. For instance, for crystallisation of polyethylene under shear, Monasse [30] has measured different growth rates in the three characteristic directions of shear. As in the present work, the highest was in the gradient direction.

3.3.3. PE3 at $T_s = 170$ °C and $T_s = 150$ °C

Figs. 7(a) and 8 show the influence of a shear rate at other shearing temperatures, 170 and 150 °C, respectively. Fig. 7(b) shows the corresponding SALS patterns for PE3 with a waiting time (t_w) of 2 s at 170 °C. As expected, the longer the relaxation times, the larger is the influence of the pre-shearing on crystallisation. Again, the apparent spherulite radius decreases due to the flow, for the same reasons as at $T_s = 190$ °C.

3.4. Influence of the shear strain for PE3 at $T_s = 170$ °C

Fig. 9(a) shows the influence of strain ($\dot{\gamma}t_s$) at 170 °C, for two shear rates (3 and 9 s^{-1}), for comparison to those investigated under constant deformation of 360 strain units (Section 3.3). Fig. 9(b) shows the corresponding SALS patterns for PE3 at $\dot{\gamma} = 9\ s^{-1}$. Clearly, there is a minimum deformation that must be applied to effectuate the influence

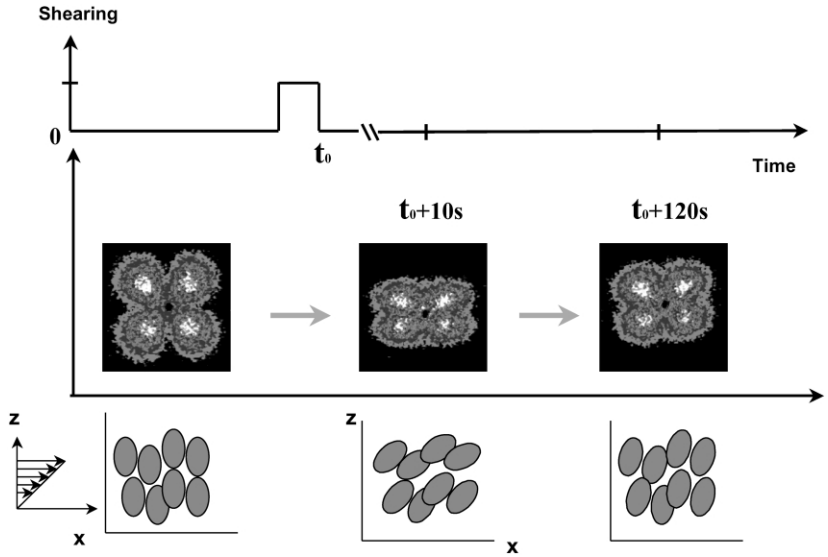

Fig. 6. Top: schematic diagram illustrating the relaxation sequence of PE3 after imposition of a deformation 'pulse' in term of a very slow relative displacement of the two plates of the shear cell at the onset of crystallisation following cooling from 190 °C. Middle: the relaxation and reversal of the SALS patterns of PE3, following its distortion by the deformation 'pulse', to its original state after few minutes. Bottom: schematic ellipsoidal morphology and explanation of the observed SALS sequence.

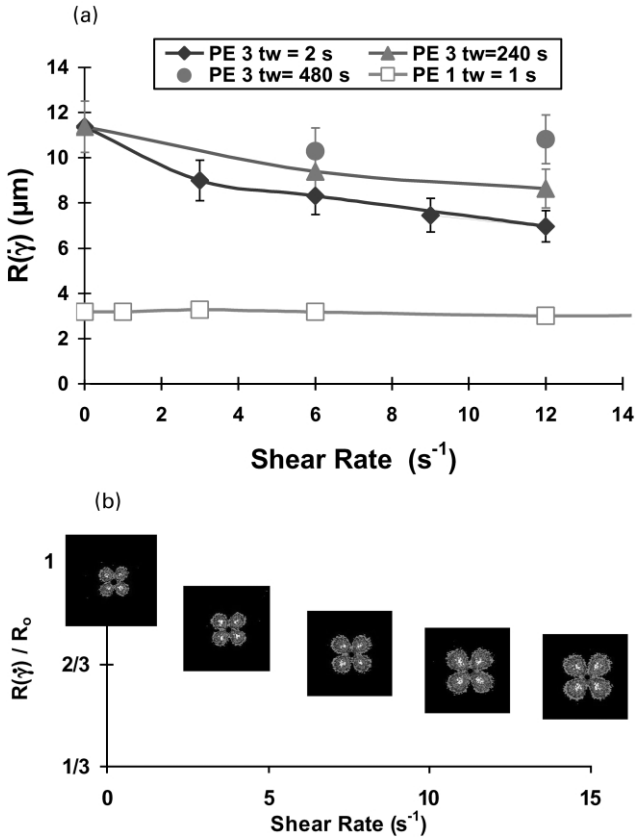

Fig. 7. (a) Spherulite radius $R(\dot{\gamma})$ versus applied shear rate for PE1 and PE3 when sheared at 170 °C, with varying length of the waiting times, t_w. (b) The corresponding SALS patterns at $t_w = 2$ s. The total deformation during shear is the same for all shear rates, i.e. $(\dot{\gamma}t_s) = 360$ shear units.

of the flow. In other words, this minimum shear strain will elongate chains long enough to prevent them from being relaxed during the experiment. This strain appears to be ~200 units for this experiment. It seems larger for the lower shear rate (~180 units, i.e. 20 s for 9 s^{-1}; and ~250 units, i.e. 80 s for 3 s^{-1}). Above this strain, the influence of the flow increases with deformation up to a limit where it saturates. Above this large shear deformation, the crystallisation will always occur in the same way, with similar time and morphological aspects. The simplest hypothesis is that shear is orienting chains more and more when deformation (or shearing time) is increased. Above that critical strain, when the longest chains are in their stable equilibrium orientation, no more change is occurring in the melt and the crystallisation will occur in the same way. This is what we

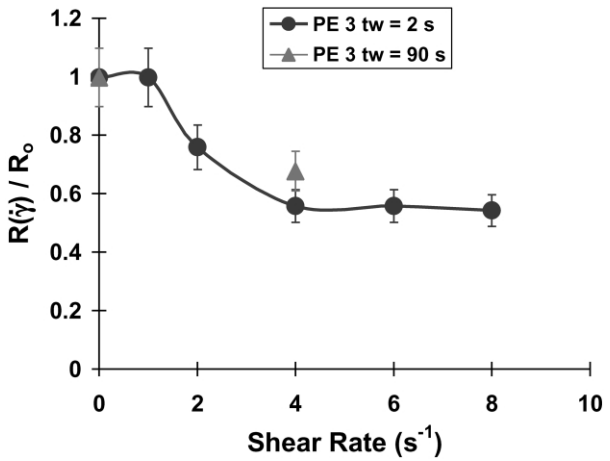

Fig. 8. Spherulite radius $R(\dot{\gamma})$ divided by the radius without shear R_0 for PE3 versus applied shear rate when sheared at 150 °C, with varying length of the waiting times, t_w. The total deformation during shear is the same for all shear rates, i.e. $(\dot{\gamma}t_s) = 360$ shear units.

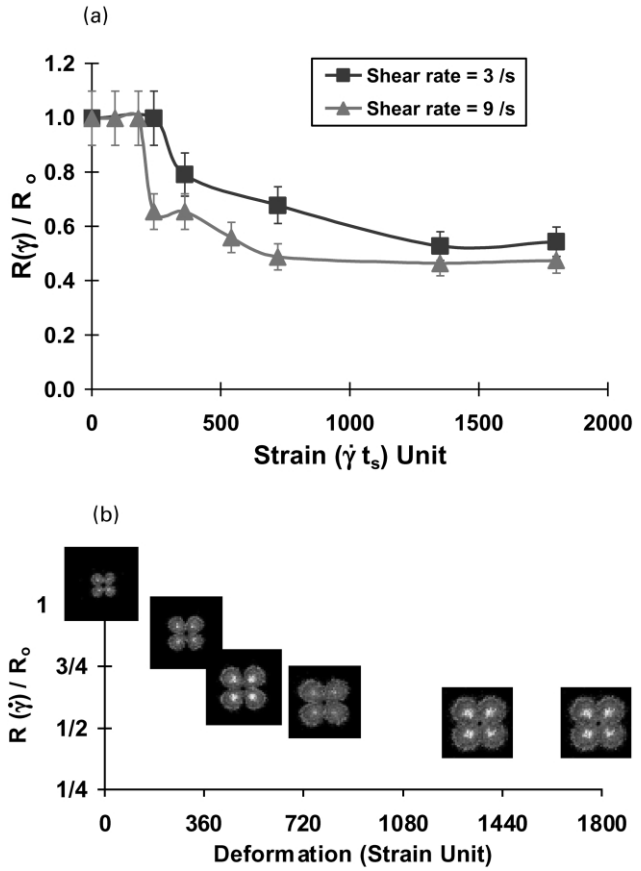

Fig. 9. (a) Spherulite radius $R(\dot{\gamma})$ divided by the radius without shear R_0 for PE3 versus deformation ($\dot{\gamma}t_s$) in strain units when sheared at 170 °C, with $t_w = 2$ s and varying level of applied shear rate ($\dot{\gamma}$). (b) The corresponding SALS patterns at $\dot{\gamma} = 9\ s^{-1}$.

observed since above around 600 strain units at 9 s^{-1} and 1200 strain units at 3 s^{-1}, the apparent radius of the crystalline structures does not change with strain any more. Again, crystallisation is a very sensitive probe for chain orientation. Looking at the rheological data, a 'steady state' would be achieved after a strain of ~50 to 100 strain units for PE3 at 170 °C. We see here that this value is too low. Shear rheology does not appear to be sensitive enough to the orientation of a small fraction of longer chains, while it is this fraction that is controlling the subsequent crystallisation processes.

It must also be noted that the strain needed to achieve an actual steady state is very high. Such long orientation times are compatible with the maximum relaxation times deduced from waiting times after shear. Such data are very important to evaluate how much strain is needed to be in a steady state regime. It seems that the critical strain depends on the applied shear rates, the lower the shear rate, the more the sample has to be sheared. This will have to be checked using more shear rates and different temperatures.

These SALS studies are consistent with the in situ, time-resolving X-ray and neutron scattering studies [36,45], which quantitatively evaluate both the development of anisotropy in sheared polymer melts and the subsequent crystal growth processes which take place on cooling from such melts. These X-ray and neutron scattering of high-density polyethylenes (HDPE) reveal the very low level of preferred segmental orientation in the sheared melt and the substantial amplification of this anisotropy through crystal growth. These work also identify the shear history required to induce anisotropic crystal growth and that this shear history requires a constant *critical shear strain* over a substantial shear rate range (10^{-2}–10^{2} s^{-1}).

3.5. Comparison of morphology on blown films

Finally, one should also ask what is the morphology of the blown film sample. Can these small-scale shear-induced crystallisation experiments capture some of the morphology created by the non-linearly, large-scale film blowing processes?

In film blowing process, the polymer undergoes shear, extensional and biaxial deformations during extrusion and bubble formation processes at above and near its melting temperature. The residual shear and extensional stresses are then relaxed before and during the subsequent crystallisation process. To address the influence of processing conditions, it is convenient to define a processing time parameter, t_p, as the time required for a polymer element to pass from the extruder exit to the frost line [46], whence crystallisation is taking place. The stresses are relaxed on a molecular time scale that is specified by a characteristic relaxation time, τ. The ratio of this relaxation time, τ, to the process time, is known as the Deborah number: ($De = \tau/t_p$) which couples the polymer molecular characteristics to the variation of processing conditions.

It has been shown [47] that *De* can be used to characterise structure–property-processing relationships of LLDPE blown films. The level of residual shear and extensional stresses that are able to relax during the melt state process will dictate the chain orientation in the finished product and therefore contribute to its solid-state morphology and physical properties. The higher the Deborah number, the higher the stresses that remain unrelaxed, leaving the *largest chains* (with the *longest* relaxation times, τ_{max}) aligned in the flow direction during crystallisation and hence controlling the degree of frozen MD/TD orientation balance on the blown films.

Fig. 10 compares the SALS patterns of PE1 and PE3 from (i) *solid* blown films of 38 μm in thickness; those re-crystallised from *melting* of (ii) base resin pellets, without pre-shearing, at 190 °C (as shown in Fig. 5(b) at $\dot{\gamma} = 0\ s^{-1}$), and (iii) the above blown films at 190 °C. Both film samples of PE1 and PE3 were blown under the same processing conditions: using a Reifenhaüser film blowing extrusion line with a 150 mm die diameter, a die gap setting of 2.3 mm, a 2:1 blown-up ratio and an extrusion output rate of 50 kg/h. These correspond to a processing time $t_p \sim 4$ s.

It can be seen in Fig. 10 that the metallocene polymer PE1 does not appear to be influenced significantly by the

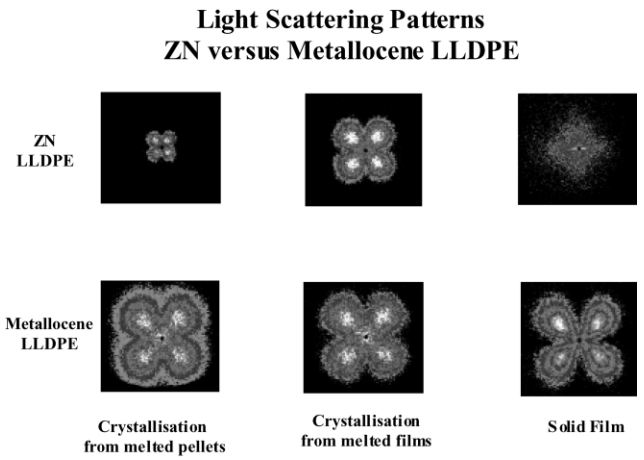

Fig. 10. SALS patterns (similar scale) of PE1 and PE3: (Right) *solid* blown films of 38 μm in thickness; (Centre) re-crystallised of the above blown films from *melting* at 190 °C; (Left) those crystallised from *melting* of base resin pellets at 190 °C, without pre-shearing (as shown in Fig. 5 at $\dot{\gamma} = 0\ s^{-1}$).

large strain, non-linear deformation during film blowing processes. This is consistent with those observed, and discussed, in Fig. 5(a) for the simple pre-shearing experiments, as the film blowing processing time is either greater, or of the order of, the largest relaxation time for this polymer ($De = \tau_{max}/t_p \sim 1$) and leads to a lack of flow memory when this narrower MWD, with a homogeneous composition, metallocene PE is crystallising.

Similarly, the very different pre-shearing behaviour as previously shown and discussed in Fig. 5(b) for the Ziegler–Natta catalysed PE3 sample has also been demonstrated in Fig. 10. The influence of the large strain, non-linear deformation during film blowing processes is very pronounced. The apparent radius of the spherulites is significantly decreased; the polymer could not have fully relaxed its orientation/deformation memory as its $De = \tau_{max}/t_p \sim 10$, which is an order of magnitude larger than that of PE1, leading to a very complex SALS pattern observed on the *solid* blown film.

4. Conclusions

The measurement of polymer relaxation time constants by probing the crystallisation kinetics is an interesting method, more sensitive than conventional rheology when a small fraction of very high molecular weight, longer chains are present in the polymer. Crystallisation kinetics is very sensitive to an applied shear, even when it has occurred some minutes before. It seems that even the presence of a minute fraction of high molecular weight chains has an important influence both on the memory of the polymer and the orientation of a subsequent crystallisation. The differences in the composition distribution between the two studied polymers would have obviously influence on their crystallisation processes, as well as on the way pre-shearing can modify crystallisation.

In turn, this would have a great importance in understanding the morphology development in polymer processing. Even if crystallisation does not take place during flow, as occurring in some parts of the mould in injection moulding, the influence of the flow history must be taken into account.

Acknowledgements

The authors thank BP Chemicals for permission to publish this work and various colleagues for helpful discussions. Financial support for a studentship at BP Chemicals, Lavéra, for Q. Auzoux is gratefully acknowledged.

References

[1] Keller A. J Polym Sci 1955;17:291–351.
[2] Fisher EW. Z Naturforsch 1957;12a:753.
[3] Keller A. Philos Mag 1957;2:1171.
[4] Till PH. J Polym Sci 1957;24:301.
[5] Lauritzen Jr. JI, Hoffman JD. J Res Natl Bur Stand 1960;64A:73.
[6] Hoffman JD, Lauritzen Jr. JI. J Res Natl Bur Stand 1961;65A:297.
[7] Hoffman JD, Frolen LJ, Ross GS, Lauritzen Jr. JI. J Res Natl Bur Stand 1975;79A:671.
[8] Hoffman JD. Polymer 1983;24:3.
[9] Pennings AJ, van der Mark JMAA, Booij HC. Kolloid Z Z Polym 1970;236:99.
[10] Keller A, Machin MJ. J Macromol Sci, Phys 1967;B1:41.
[11] Hill MJ, Keller A. J Macromol Sci, Phys 1969;B3:153.
[12] MacHugh AJ, Forrest EH. J Macromol Sci, Phys 1975;B11:219.
[13] Haas TW, Maxwell B. Polym Engng Sci 1969;9:225.
[14] Kobayashi K, Nagasawa J. J Macromol Sci, Phys 1970;B4:331.
[15] Wereta A, Gogos C. Polym Engng Sci 1971;11:19.
[16] Krueger D, Yeh GSY. J Appl Phys 1972;43:4339.
[17] Fritzsche AK, Price FP. Polym Engng Sci 1974;14:401.
[18] Fritzsche AK, Price FP, Ulrich RD. Polym Engng Sci 1976;16:182.
[19] Lagasse RR, Maxwell B. Polym Engng Sci 1976;16:189.
[20] Tan V, Gogos C. Polym Engng Sci 1976;16:512.
[21] Sherwood CH, Price FP, Stein RS. J Polym Sci, Polym Symp 1978;63:77.
[22] Wolkowicz MD. J Polym Sci, Polym Symp 1978;63:365.
[23] Chang EP, Kushner B. Polym Engng Sci 1979;19:16.
[24] Chien MC, Weiss RA. Polym Engng Sci 1988;28:6.
[25] Moitzi T, Skalicky P. Polymer 1993;34:3168.
[26] Tribout C, Monasse B, Haudin JM. Colloid Polym Sci 1996;274:197.
[27] Vleeshowers S, Meijer HEH. Rheol Acta 1996;35:391.
[28] Nieh JY, Lee LJ. Polym Engng Sci 1998;38:1133.
[29] Wang C, Liu CR. J Polym Sci, Polym Phys 1998;36:1361.
[30] Monasse B. J Mater Sci 1995;30:5002.
[31] Monasse B. Mater Sci 1992;27:6047.
[32] Varga J, Karger-Kocsis J. J Polym Sci, Polym Phys 1996;34:657.
[33] Jay F, Haudin JM, Monasse B. J Mater Sci 1999;34:2089.
[34] Liedauer S, Eder G, Janeschitz-Kriegl H, Jerschow P, Geymayer W, Ingolic E. Int Polym Process 1993;8:236.
[35] Kumuraswamy G, Issaian AM, Kornfield JA. Macromolecules 1999;32:7537.
[36] Pople JA, Mitchell GR, Chai CK. Polymer 1996;37:4187.

[37] Chai CK, Dixon NM, Gerrard DL, Reed W. Polymer 1995;36:661.
[38] Lesec J. J Liq Chromatogr 1994;17:1029.
[39] Glockner G. J Appl Polym Sci 1990;45:1.
[40] Stein RS, Rhodes MB. J Appl Phys 1960;31:1873.
[41] Baumgartel M, Winter HH. SPE Tech Papers 1989;35:1652.
[42] Chai CK. Unpublished data.
[43] Hsiao BS, Somani R. Conference presented at the International Workshop on Scattering Studies of Mesoscopic Scale Structure and Dynamics in Soft Matter, Messina, Italy; November 22–25, 2000.
[44] Haudin JM, Monasse B. In: Cunha AM, Fakirov S, editors. Structure development during polymer processing. Dordrecht: Kluwer Academic Press; 2000. p. 47.
[45] Holt JJ, Mitchell GR, Chai CK. Crystallization from sheared melts of linear and branched polyethylenes. Proceeding of EPS Conference, Hungary; September 2001.
[46] Shirodkar PP, Firdaus V, Fruitwala H. Plast Engng 1994;9:27.
[47] Chai CK. Influences of molecular weight distribution and processing conditions on LLDPE blown film property. Proceeding of Polymer Processing Society 18th Annual (PPS-18) Conference, Portugal; June 16–20, 2002.